



HAL
open science

A hygro-mechanical analysis of poplar wood along the tangential direction by restrained swelling test

Paola Mazzanti, Julien Colmars, Joseph Gril, David Hunt, Luca Uzielli

► To cite this version:

Paola Mazzanti, Julien Colmars, Joseph Gril, David Hunt, Luca Uzielli. A hygro-mechanical analysis of poplar wood along the tangential direction by restrained swelling test. *Wood Science and Technology*, 2014, 48 (4), pp.673-687. 10.1007/s00226-014-0633-4 . hal-01295539

HAL Id: hal-01295539

<https://hal.science/hal-01295539v1>

Submitted on 31 Mar 2016

HAL is a multi-disciplinary open access archive for the deposit and dissemination of scientific research documents, whether they are published or not. The documents may come from teaching and research institutions in France or abroad, or from public or private research centers.

L'archive ouverte pluridisciplinaire **HAL**, est destinée au dépôt et à la diffusion de documents scientifiques de niveau recherche, publiés ou non, émanant des établissements d'enseignement et de recherche français ou étrangers, des laboratoires publics ou privés.

A hygro-mechanical analysis of poplar wood along the tangential direction by restrained swelling test

Paola Mazzanti · Julien Colmars · Joseph Gril · David Hunt · Luca Uzielli

Abstract A better understanding of the hygro-mechanical behaviour of poplar wood (*Populus alba* L.) is proposed by means of restrained swelling tests. Small clear specimens were tested along their tangential direction in controlled climatic conditions; a dry climate (30 % relative humidity and 30 °C temperature) and a humid one (80 % relative humidity and 30 °C temperature) were cyclically set and kept constant each during 7 days. In these conditions, three matched specimens were tested at the same time along the tangential direction: specimen A free to shrink and swell, specimen B free to shrink and prevented from swelling beyond its initial dimension, specimen C prevented from shrinking and swelling. A specific device was set up to monitor strain and/or stress on each specimen. During the adsorption phase, compression forces (on specimens B and C) were measured, and during the desorption step, compression set shrinkage (compression strain at zero load) and tension stress (on specimens B and C, respectively) were measured. In this paper, the dedicated experimental device is presented and a deep analysis of experimental curves is then proposed by means of a rheological approach. By the analysis, some basic data are obtained (swelling coefficient, swelling pressure and compression set shrinkage), and a complex behaviour of wood made of reversible and irreversible phenomena is characterized.

P. Mazzanti (✉) · L. Uzielli
GESAAF, University of Florence, Florence, Italy
e-mail: paola.mazzanti@unifi.it

J. Colmars · J. Gril
LMGC, University Montpellier 2, Montpellier, France

D. Hunt
University of Reading, Reading, UK

Introduction

Compression set and swelling pressure

In wood, strain due to the swelling/shrinkage of the material perpendicular to the grain is much larger than the mechanical strain commonly encountered during short- and long-term loading tests. From oven dry to fibre saturation point (FSP) condition, common woods could swell up to 10 % (Tiemann 1942), whereas mechanical strain due to external loading is of an order of magnitude lower in the linear domain 0.1–0.2 % (Hoadley 1995). Thus, when wood is restrained from swelling and shrinking across the grain, a large stress and nonlinear moisture-dependent behaviour occur due to restrained strain.

Preventing a piece of wood from swelling is an easy test to set up. During such a test, several authors have observed a residual compression strain and named it ‘compression set’ (Tiemann 1942; Buck 1963; Hoadley 1969, 1995). The occurrence of residual strain in similar conditions was also observed in tension by Tiemann (1942), Takahashi and Schniewind (1974), respectively, called tension set.

The maximum stress that occurs in wood during restrained swelling has been called ‘swelling pressure’ or ‘swelling stress’ and investigated by many researchers (Barkas 1949; Bolton et al. 1974; Mishiro 1988; Molinski and Raczkowski 1988; Perkitny 1961; Perkitny and Kingston 1972; Rybarczik and Ganowicz 1974). Other researchers (Hoadley 1969; Takahashi and Schniewind 1974) were more interested in the residual strain after restrained swelling than in the maximum stress developed by the material.

The reasons for investigating wood compression set and/or wood swelling stress are very different from one author to another: wood densification (Blomberg and Persson 2007), durability of wooden floors and structural elements (Perkitny 1961), wooden panels for buildings (Virta et al. 2005) and conservation of wooden objects from cultural heritage (Hoadley 1995; Buck 1963). It is known that for a panel painting, the presence of a paint layer on one side only causes an asymmetric moisture exchange. In addition, the restrained swelling is a likely condition to occur because of the constructive feature of the panel paintings, and it is responsible for high stress levels, which in turn cause the compression set deformation. It shows up as a loss of dimension and computed as a percentage of the original dimension. Since the 1960s (Buck 1963), this deformation is considered the main cause producing the warping of the panel paintings that, in the literature, is usually identified as permanent. Actually, a permanent phenomenon lasts as long as the actions that produce it persist, and reversible and/or irreversible effects could show up when such actions cease. In order to avoid misunderstanding, for this paper, the concepts of reversible (elastic deformation, part of mechano-sorptive and visco-elastic creep, part of compression set shrinkage) and irreversible (part of mechano-sorptive and visco-elastic creep, damage, plastic deformation, part of compression set) phenomena are used.

The warping of the panel paintings shows up when the wooden support is in equilibrium with the climatic conditions, and no moisture gradient is present across the panel thickness. According to Buck (1963), such deformation has to be considered a compression set shrinkage on the back of the panel. Also, Hoadley

(1995) proposed such hypothesis as an explanation of the panel painting warping, suggesting an experimental test (see ‘[The test procedure proposed by Hoadley](#)’).

The test procedure proposed by Hoadley

According to Hoadley, the basic principle consists in selecting three matched specimens subjected to the same moisture cycling and to three different boundary conditions (Fig. 1). Everything here is considered as a one-dimensional mechanical effect. Specimen A is free to swell and shrink, specimen C is fully restrained and specimen B is an intermediary condition in which only swelling beyond its initial dimension is prevented.

The experiments are based on the one proposed by Hoadley and will be described in the following (see ‘[Mechanical testing](#)’).

Due to the mechanical couplings between stress, strain and moisture variations in wood, Hoadley (1995) expects specimen B to show residual deformation named compression set (CS) after the first adsorption–desorption cycle. Moreover, he supposes that specimen C will probably crack (Fig. 1) because of its specific boundary condition. Indeed, Hoadley specifies that when relative humidity (RH) changes from 20 up to 80 %, unrestrained panels of poplar wood should swell up to approximately 3 % along the tangential direction. Thus, considering a restrained panel (as in a frame), the whole 3 % swelling deformation is prevented. When the panel gets back to the initial humidity condition, it recovers approximately 1 %, that is, the elastic limit for short-term mechanical loading across the grain, while the remaining 2 % is the expression of compression set.

In the literature, no evidence of such a test or similar applied to the conservation of panel paintings is present.

Work plan and aims

In the same way as Hoadley (1995), the authors focused on the objective of understanding and modelling the response to climatic variations in historical panel

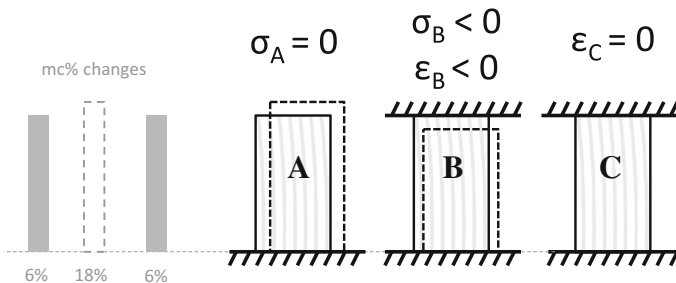


Fig. 1 Compression set experiment in tangential direction as proposed by Hoadley. Three matched wood specimens are subjected to a moisture content cycle between 6 and 18 %. Specimen A is free to swell and shrink, C is prevented from doing so, whereas B is only prevented from swelling beyond its initial size. Adapted from Hoadley (1995)

paintings; thus, it was proposed to investigate the hygro-mechanical behaviour of wood under restrained swelling by focusing, not only on swelling pressure and residual strain, but also on stress–strain behaviour and its kinetics during the test. It represents a part of a larger work that includes material characterization, rheological modelling, structural (panel) modelling and panel monitoring.

In this paper, an apparatus specifically developed in order to reproduce Hoadley's test in the tangential direction with a strain–stress monitoring is presented. Poplar wood (*Populus alba* L.), which is known to have been widely used as painting support in Central Italy from the twelfth to sixteenth century (Uzielli 1995), was chosen for the experiments. Wood is a natural composite reinforced by cellulose fibres and is highly anisotropic; for small specimens taken far from the pith, it can be considered orthotropic. The tangential direction combines both the highest swelling–shrinkage coefficient (α) and the lowest elastic modulus (E) compared with the radial and longitudinal directions. Even if swelling pressure ($E^*\alpha$) is expected to be isotropic in wood (Preziosa et al. 1986), tangential direction has been chosen to obtain as large as possible deformations.

Several authors carried out tests on swelling pressure (Perkitny 1961; Krauss 2004; Virta et al. 2006) or on compression set (Tiemann 1942; Buck 1963; Hoadley 1969; Takahashi and Schniewind 1974). The test here proposed is more oriented towards the analysis of compression set that can occur naturally and concerning the conservation of panel paintings. From here, the importance of performing the tests on three hygroscopic cycles can be seen, which should lead to a better understanding of time- and moisture-related effects. Furthermore, the analysis of the wood behaviour during the test is here investigated more than the study of the compressed wood properties. The test results (strain and stress) were presented and processed to characterize some of the hygro-mechanical aspects that influence the panel paintings conservation.

Materials and methods

Material

A batten was cut from a plank of poplar sapwood (density 390 kg/m^3 , at 12 % moisture content (MC)), approximately $1000 \times 30 \times 50 \text{ mm}^3$ ($L \times R \times T$), and stored (for organizational reasons) in a climatic chamber set to standard conditions (65 % RH and 20 °C) for 1 year. Thirty clear specimens were cut from the equilibrated batten, their dimensions being approximately $10 \times 20 \times 40 \text{ mm}^3$ ($L \times R \times T$), and were stored in a climatic chamber set to 30 % RH and 30 °C (which in this paper is defined as a dry climate) for 3 months, values representing the initial environmental conditions for all the tests reported here. According to the standard UNI ISO 3130, the specimens were periodically weighed until they reached a constant value and the new equilibrium moisture content (EMC) was calculated for some of them, giving an average value of 6.3 %.

In the dry climate conditions, the specimen density was calculated (see Table 1) and used to verify the matching of the cut-next-to-each-other specimens.

Table 1 Average dimensions, density and annual ring width of the cut specimens

| Specimen measured | L (mm) | R (mm) | T (mm) | Dry condition density (kg/m ³) | Annual ring width (mm) |
|-------------------|----------|----------|----------|--|------------------------|
| 19 | 10.25 | 18.75 | 39.90 | 370 | 8.90 |

Table 2 RH variations, maximum free swelling strain measured for specimens A and B, maximum compression stress (swelling pressure) measured for specimens B and C (they showed the same swelling pressure during the compression phases) for the performed tests

| RH variations (%) | Min $\sigma^{B,C}$ Swelling pressure (MPa) | Max $\Delta\epsilon^A$ | Max $ \Delta\epsilon^B $ |
|-------------------|---|------------------------|--------------------------|
| 27-82-27 | -1.1 | 0.025 | 0.015 |
| 34-78-34 | -1.2 | 0.026 | 0.015 |
| 30-77-30 | -1.0 | 0.020 | 0.023 |
| 30-77-30 | -1.0 | 0.025 | 0.023 |

Climate cycling

The temperature (T) was set to a constant value of 30 °C in order to speed up the adsorption/desorption processes, and the RH varied cyclically between approximately 30 and 80 % (see Table 2). Each adsorption/desorption phase lasted 7 days, which is the time for the specimens to reach the new EMC (checked by weighing dummy specimens kept in the same environment), and repeated three times for each test (Fig. 2). A data logger (HOBO U12-013 by Onset) was used to monitor T and RH, acquisition 5 min. In these climatic conditions, the assumed average MC of the tested specimens cycled between 6.3 and 15.3 %, calculated by weighing the dummy specimens, named D.

Mechanical testing

The test equipment was designed at GESAAF (at that time DISTAF) laboratories and fabricated in a local workshop. It consists of three devices (Fig. 3) made from aluminium and stainless steel parts, each one able to guarantee the chosen degree of freedom:

- device A allows the specimen A to deform freely; the two extreme bars are fixed, while the central one slides on the rods guided by low friction bearings, following the specimen shrinkage and swelling;
- device B has fixed extreme bars and a sliding central one, also guided by low friction bearings; the central bar can move down the rods following the specimen shrinkage and cannot move up the rods due to hard-set screws that block it, preventing the specimen B from swelling beyond its initial dimension;
- device C guarantees that the specimen C cannot deform, thanks to hard-set bars.

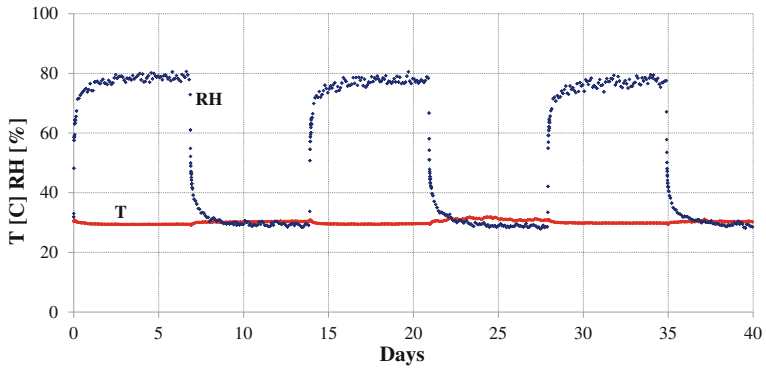


Fig. 2 Climatic conditions, relative humidity (*RH*) and temperature (*T*) set in the climatic chamber to carry out the experimental tests

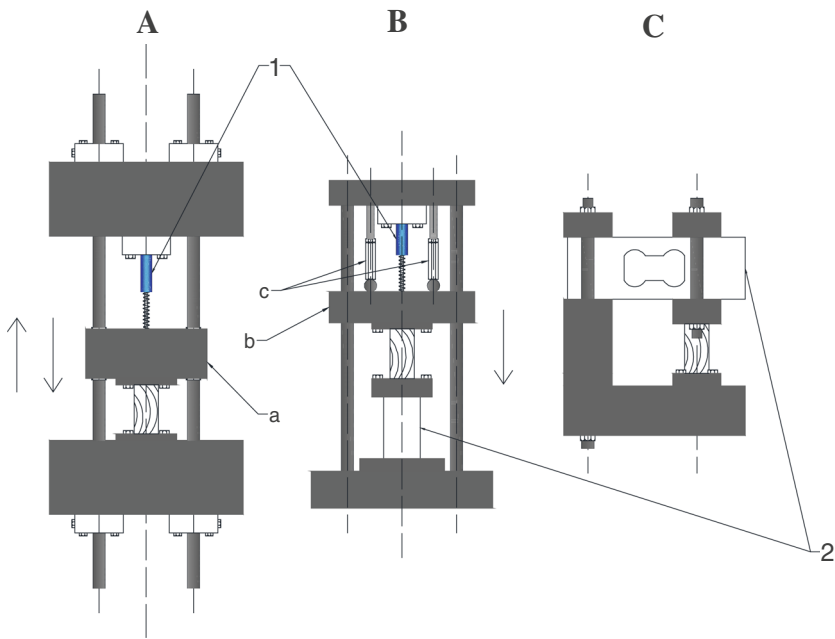


Fig. 3 Testing devices designed for restrained swelling tests. Device **A** measures free swelling and shrinkage of sample **A** using a linear transducer (1), device **B** measures the free shrinkage using a linear transducer (1), the compression stress during the adsorption phase using a load cell (2) and device **C** measures the compression and tension stress using a load cell (2). (*a*) and (*b*) are the aluminium *bars* sliding along the *rods*, (*c*) the hard-set screws. The *arrows* illustrate the central *bar* sliding for devices **A** and **B**

The specimens were glued on aluminium plates by means of a structural epoxy resin that was spread in a thin layer of approximately 50 μm . Twenty four h passed before the test began for the resin setting. Local boundary constraints due to the gluing of specimens on metal plates were ignored.

Being glued to the sliding bars, the end-faces of the specimens were prevented from rotating and from shifting laterally.

The specimens were tested along their tangential direction, while the longitudinal and radial directions were completely free to deform and were not measured.

The tests were carried out with the devices horizontally placed so to avoid gravity effects.

Results and discussion

The whole test was repeated on four different groups of specimens A, B, C (Table 2). All groups indicated the same kind of mechanical response, so only one of them, i.e. test #4, will be discussed in detail (Table 3), except for the deformation of specimen B. Indeed, the CS measures are not reliable because of technical problems, and in replacement, data from test #1 are shown. Moreover, these deformation data are analyzed only in section 'Results versus time', and do not influence the analyses presented in other parts of this paper.

Results versus time

For the test #4, the results of strain and stress are plotted against time (Fig. 4). The MC of specimen A clearly follows the relative humidity variations in the climatic chamber. Since the present analysis assumes that in every moment, MC is the same for the three specimens, the free swelling/shrinkage of specimen A is also used as a reference for specimens B and C of the same group.

The free swelling of specimen A from 6.3 to 15.3 % MC is 2.5 % along the tangential direction, with a swelling rate of approximately 0.28 %/%. The free shrinkage is 2.4 %, with a shrinkage rate of approximately 0.26 %/%. The slight difference between swelling and shrinkage should be attributed to the hysteresis and the RH inaccuracy of the chamber.

During the first adsorption phase, B and C specimens are put into a compression state, and a negative stress level is measured. During the following desorption, the behaviour of the specimens shows up through both strain and stress: B starts shrinking to below its original dimension and C shows tensile stress (Fig. 4, positive stress). Similar behaviour continues over the subsequent cycles.

Table 3 Climatic conditions of test #4 for each cycle

| | 1st cycle | | 2nd cycle | | 3rd cycle | |
|------------|----------------|------------------------|----------------|------------------------|----------------|------------------------|
| | RH average (%) | Standard deviation (%) | RH average (%) | Standard deviation (%) | RH average (%) | Standard deviation (%) |
| Adsorption | 78 | 1.96 | 77 | 1.72 | 76 | 2.00 |
| Desorption | 30 | 0.99 | 30 | 1.26 | 30 | 1.25 |

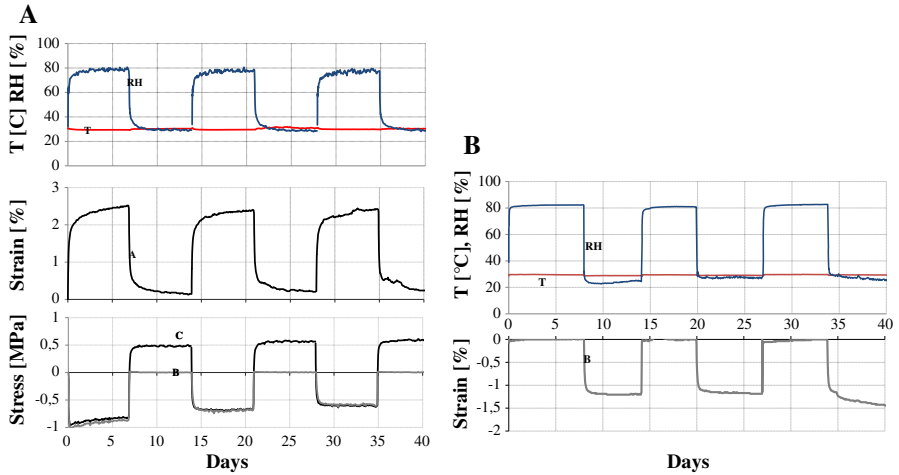


Fig. 4 **a** Results from test # 4. The climatic conditions set in the chamber, the strain (%) and the stress (MPa) measured on specimens A and C are plotted versus time. Tension stress is +, swelling is increasing and shrinkage is decreasing. No deformation data of specimen B are shown because of technical problems of the measurement apparatus; in their place, deformation data of specimen B are here presented for test #1. **b** Results from test # 1. The climatic conditions set in the chamber, and the strain (%) measured on specimen B are plotted versus time. Tension stress is +, swelling is increasing and shrinkage is decreasing

During the desorption phase, the compression set is measured on specimen B as the maximum loss of dimension when the equilibrium is reached. During the 1st cycle, it is -1.20% ; during the 2nd cycle, it is -1.18% ; and during the 3rd cycle, it is -1.42% (the value is reported even if the RH is not well controlled during the 3rd desorption phase and influences the measure, as shown in Fig. 4b). Such residual strain ε_r (Table 2) is 0.019 on average, a high value comparable with the hygroscopic strain (0.024 on average). According to Svensson and Toratti (2002), the mechano-sorptive strain is less than half of the hygroscopic one, and for the test, it is calculated as 0.010. It confirms that the measured residual deformation is in part a mechano-sorptive effect and in part a compression set shrinkage. As for the stress, for the sake of simplicity, it is calculated considering the cross-section area constant for both the specimens. For the first absorption phase, the stress curves show the following behaviour, which does not appear in the subsequent ones; compression stress reaches rapidly (after 330 min) a maximum absolute value (1.0 MPa) and then decreases while MC is still increasing. The stress has decreased by around 23 % after 150.5 h from the peak. The second and third absorption phases exhibit practically constant stress, with an average maximum absolute value of 0.7 and 0.6 MPa, respectively. Such fact underlines the importance of performing this kind of test on more than one sorption cycle.

When the specimen is also prevented from shrinking (curve C), tension stresses are present, and no relaxation effect is evident even during the first desorption phase. Cycle after cycle the average maximum tension stress increases from 0.47 to 0.57 and to 0.59 MPa.

Graphing the stress–strain diagrams

In order to plot and analyze the data obtained from this test, the basic assumption is made that the data from the three specimens A, B and C can be directly related to each other, since the material may be assumed identical and subjected to identical moisture cycling. To this purpose, the following further assumptions need to be made.

- a. The strain of each specimen can be split into independent parts, which are:
 - mechanical strain ε_m , related to stress σ throughout the constitutive law,
 - hygroscopic strain $\varepsilon_\alpha = (mc - mc_0)\alpha$ (independent from stress, see next assumption), where mc_0 is a random reference value, and α is the swelling (shrinkage) coefficient.

Thus, the total strain ε is:

$$\varepsilon = \varepsilon_m + \varepsilon_\alpha \quad (1)$$

This is of great interest for certain configurations, such as for C specimen which boundary conditions are $\varepsilon = 0 \Rightarrow \varepsilon_m = -\varepsilon_\alpha$.

For wood material, ε_m is generally split into the following parts: elastic strain ε_e ; viscous strain ε_v ; mechano-sorptive strain ε_{ms} ; and residual strain ε_r , which will be discussed as compression set next.

Total strain of each specimen $X(= A, B, C)$ is then written as:

$$\varepsilon^X = \varepsilon_\alpha^X + \varepsilon_e^X + \varepsilon_v^X + \varepsilon_{ms}^X + \varepsilon_r^X \quad (2)$$

- b. The coupling between stress and EMC will be neglected here.

Stress and moisture expansion are probably coupled in wood material. According to Barkas (1949), and Simpson and Skaar (1968), wood specimens under compressive stress reach slightly lower moisture content than nonstressed specimens. From the literature, it is hard to estimate this effect on wood stressed in tangential direction. Because of lack of data on the material here, the coupling between stress and moisture equilibrium will be neglected.

It is assumed that the governing equation for the material is of type:

$$\sigma = K_T(\varepsilon - \varepsilon_\alpha) \quad (3)$$

where K_T can be read graphically as a tangent rigidity, including time and moisture-dependent effects.

- c. Swelling/shrinkage strain is independent from external stress, thus at any time:

$$\varepsilon_\alpha^A = \varepsilon_\alpha^B = \varepsilon_\alpha^C \quad (4)$$

This assumption is maintained, although at least one example of coupling between stress and moisture-induced strain is given by Hunt and Shelton (1988)

where for softwood, a reduction in longitudinal swelling/shrinkage coefficient under stress had to be assumed to explain the observed response in bending with subsequent moisture variation after reaching the creep limit (Hunt and Shelton 1988; Hunt 1999). However, the error implied by maintaining such assumption is here considered negligible.

The following consequences can be drawn from the above assumptions.

Because of specific boundary conditions, at any time $\varepsilon^C = 0$. For specimen B, the relation is $\varepsilon^B \leq 0$ and in particular, $\varepsilon^B = 0$ if one considers only the instants when B exhibits compression stress. Thus, it is possible to calculate ε_m^B from Eqs. (1) and (4) at any time of the experiment by measuring the free strain of specimen A and the compressive strain of specimen B. The same applies to specimen C.

The response of specimens B and C is analyzed in the following by means of a stress–strain representation method used by Mishiro (1976) and Krauss (2004). Such representation shows $\sigma^{B,C}$ versus $-\varepsilon_\alpha^A = -\varepsilon_m^{B,C}$, as in a conventional stress–strain curve (Fig. 5).

Discussing the stress–strain diagrams

This section discusses the hygro-mechanical behaviour shown by specimens B and C during the performed tests, and some conclusions which can be hence derived by commenting Fig. 5a, b. Such figures do not show explicitly the progression of time nor the MC of the specimens, which changes with time, being produced by the imposed RH cycling. The time and RH values corresponding to a given point on stress–strain diagrams will be here referred to with reference to Fig. 4, and MC values will not be mentioned, since in fact they could not be regularly measured during the tests.

The curves describing the 1st, 2nd and 3rd cycle are shown together and can be identified by the specific symbols. The curves follow a clockwise loop. In order to

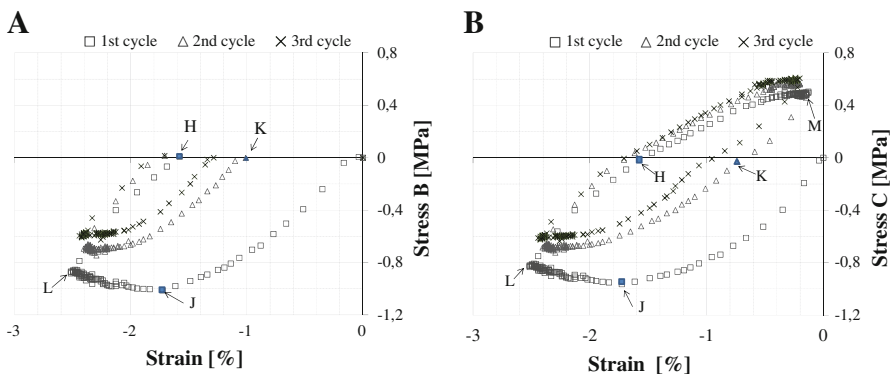


Fig. 5 Stress strain diagrams where **a** shows the B stress versus minus-A-strain and **b** shows the C stress versus minus-A-strain. The symbols indicate: (*square*) 1st cycle, (*triangle*) 2nd cycle and (*times*) 3rd cycle. 0H is the compression set, and 0K is the loss of dimension of specimens B and C. Point J identified the stress peak, point L the end of the first absorption phase and point M (5b) the end of the 1st cycle and the starting of the 2nd one

facilitate their description, some remarkable points are identified by symbols, for the sake of simplicity just for the first cycle.

Partially restrained test: specimen B (Fig. 5a)

The first adsorption phase is represented by the OJL curve.

When the adsorption starts and the MC increases, a growing compressive state develops in wood (curve OJ). At the same time, wood also exhibits some relaxation effects that contribute to reduce the stress; the specimen shows a complex mechanical behaviour composed of an elastic deformation produced by the increasing MC, together with a stress relaxation (in part visco-elastic and in part mechano-sorptive), growing with the increasing stress; possibly some plastic effects and/or damages of the material are also present. At point J, a stress peak shows up, and the relaxation starts prevailing over the growing stress; this happens when the RH is ca. 70 %, and 330 min have elapsed since the beginning of the test. Such point corresponds to the moment when the rate of MC increase slows down.

The strain rate clearly decreases, and the measured strain coincides with 67 % of the maximum strain; thus, this time could be considered as a characteristic time.

After 168 h (point L), the desorption phase of the cycle gets started, and the compressive state starts decreasing. Thus, the stress recovery is visible (curve LH), produced by the decrease of RH.

When the stress reaches zero (point H), there is no more stress recovery, because the specimen B is free to shrink; the loop is closed by the segment HO that represents the strain recovery 'epsilon a', which can be considered to somehow represent the compression set. The point H corresponds to an RH value of ca. 60 % and 50 min elapsed since the beginning of the desorption phase.

By simply observing the number of experimental points forming each length unit of the curves and knowing that the time interval between such points is constant, one can estimate the duration of each part, and hence predict the prevailing mechanism acting where points are far from each other; the changes are quite quick, and one may assume that the reaction is mainly mechano-sorption, whereas when points are extremely numerous and close to each other, then visco-elastic mechanisms might prevail; all the more that a definite change of strain rate can be observed between the two main parts of each curve.

The second adsorption phase starts from point O, and the loss of dimension is readable in Fig. 5a as the segment OK. As a consequence, an increase of the density could be observed. Again the stress increases following the humidification, but different to what was described for the first cycle, it shows no intermediate peak value.

The third cycle is comparable with the second one, and the same description could be applied.

Further comments can be added:

- the first cycle covers a larger area than the two subsequent ones; a possible explanation could be a damage of the material, due to the compression state, the

specimen undergoes during the adsorption phase and that could cause a reorganization at the ultrastructural level;

- the areas represent the energy spent during each cycle that from an initial value decreases approaching a minimum; the system reaches a new equilibrium condition—either in anatomical changes or rheological behaviour—adapting to minimum energy responses to similar environmental stresses.

Completely restrained test: specimen C (Fig. 5b)

Specimen C behaves like specimen B for the compression phases (adsorption), and the same comments apply. On the contrary, during the desorption phase, the specimen firstly releases the compressive state and afterwards undergoes a tension state. Again, the CS could be read as the segment OH, representing the state when the specimen is in a zero-load condition during the first desorption phase. When the dry equilibrium condition is reached (point M), a residual tension stress of the material is measured (higher for the first cycle than for the two subsequent ones). Such residual tension stress quantifies the tendency of specimen C to reduce its original dimension. The second adsorption phase starts in point M, and the loss in dimension is represented by the segment OK, when the specimen is in a zero-load condition. The small gap between point M and the Y axis can be attributed to both the hysteresis of the specimen A and the slight inaccuracy of the chamber's climatic conditions.

Further comments can be added:

- specimen C shows the same behaviour as B, that is, the compression loading at high MC values is more crucial than the tension loading at low MC, whose effects have to be considered negligible;
- the specimen never cracks during the desorption phase. When RH is equilibrated, the average stress (0.48 MPa) is approximately 15 % of the strength (Mazzanti et al. 2012) and although it lasts for 152 h, it does not produce any cracks in the wood.

Starting a numerical model for the described tests

Describing the material's stress–strain relationship is a basic prerequisite in order to lay down any mathematical model, and this section intends to discuss and quantitatively demonstrate that the elastic behaviour is one of the components of the phenomenon together with relaxation mechanisms (both visco-elastic and mechano-sorptive), plastic effects and damage.

The analysis of Fig. 5b highlights specific parameters, for the sake of simplicity, only the first cycle is discussed:

- the maximum stress in tension (point M);
- the slope of the initial part of the curve during the first absorption phase (rigidity);
- the compression set as the segment OH.

The tension stress measured on specimen C (approximately 0.5 MPa) equals the compression set deformation on specimen B (approximately 1.2 %), because they are two aspects of the same phenomenon. If no damage or creep deformation occurs after the first cycle, the residual tension stress should result in elastic deformation only. So according to Hooke's law, the stress corresponding to the measured compression set is 1.5 MPa (the rigidity is 129 MPa, see section '[Degradation of material properties](#)'); on the other hand, the measured stress is only one-third of the computed one. It confirms that the elastic deformation is not the only phenomenon involved and that a significant part of the stress (2/3) is not shown and is (temporarily) stored in the material without any external macroscopic stresses and can be recovered by further moisture cycling.

Degradation of material properties

In the stress–strain graph (Fig. 5), the response of wood to a rapid relative humidity change and/or small time scale is more visible than in the time representation (Fig. 4). Therefore, it is here used to discuss the short-term properties of specimen C. In order to estimate the degradation of the material, the rigidity of the 1st absorption phase is computed and compared with the rigidity of the 2nd one. If damage occurs, decreasing of a rigidity value should be observed, supposing the specimen was initially free from damage.

During the experimental test, the strain and stress data were recorded at a rate of 1 point/min (whereas stress/strain graphs of Figs. 4 and 5 have been plotted with 1 point every 10 min). By calculating stress rate over strain rate, tangent rigidity was obtained at any time; then, average rigidity was calculated over 10 min at different moments of the test: initial time, start of second and start of third adsorption phase. The name rigidity is here preferred to elastic modulus due to the duration of both data acquisition step (1 min) and time chosen for averaging process (10 min); moreover, the tangent rigidity might include short-term visco-elastic and mechano-sorptive effects and should not be considered as the elastic modulus of the material.

The rigidity is calculated as 129 MPa for the first cycle, 112 MPa for the second and 112 MPa for the third one; thus, a decrease of 13 % is observed from the 1st cycle to the 2nd cycle. From the first desorption, rigidity has clearly dropped that implies a damage of wood. During the following cycles, rigidity remains almost constant with the exception of natural variations with moisture content. This fully supports the idea the damage occurs during the first absorption phase due to high compressive loading.

For these tests, the rigidity is definitely a function of the time because of the viscous phenomena. Here, it is chosen to compute it between the 5th and the 15th minute since the starting that leads to the above described results. However, such dependence needs an in-depth analysis.

Conclusion

Restrained swelling tests have been performed on poplar wood in tangential direction. A specific apparatus was developed in order to test matched specimens

under different boundary conditions ($[\sigma = 0]$, $[\varepsilon \leq 0, \sigma \leq 0]$), $[\varepsilon = 0]$ and get a continuous stress–strain monitoring. Data-sets were obtained over various moisture cycles, for a total duration of 42 days. Swelling pressure of poplar in tangential direction was approximately 1 MPa, when temperature was 30 °C and humidity varied between 30 and 80 %.

The restrained swelling data were processed using stress/strain representations, and the underlying assumptions on the material behaviour (such as the swelling independent from the stress) were introduced. It allowed to describe the hygro-mechanical behaviour of poplar wood as being composed of a stress increasing due to the humidification together with a compression stress relaxation. During the desorption phase, the compressive stress decreases up to a zero-load condition that for specimen B (free to shrink and prevented from swelling) results in compression set shrinkage and for specimen C (prevented both from shrinking and swelling) in tension stress. The test, also highlights that notwithstanding specimens B and C are subjected to different boundary conditions, their behaviour is perfectly comparable both quantitatively and qualitatively cycle after cycle because the compression loading at high MC value is more important than tension loading at low MC values.

This research could add some information focused on the painted panels conservation. Indeed considering that a panel painting could be subjected to various constraint conditions (frames or crossbeams); according to this research, the mechanical effects are comparable because it is the compression state that produces damages and deformations. The wooden support undergoes the greater alterations during the first adsorption phase, of course if the subsequent cycles are comparable, or better during each first cycle, the wooden support is subjected.

Acknowledgments The Authors would like to acknowledge the COST Action IE0601 for the networking.

References

- Barkas WW (1949) The swelling of wood under stress; a discussion of its hygroscopic, elastic and plastic properties, based on a course of lectures given at Svenska träforskningsinstitutet, Stockholm, Sweden, March 1948. H.M. Stationery Off, London
- Blomberg J, Persson B (2007) Swelling pressure of semi-statically densified wood under different mechanical restraints. *Wood Sci Technol* 41:401–415
- Bolton AJ, Jardine P, Vine MH, Walker JCF (1974) The swelling of wood under mechanical restraint. *Holzforschung* 28:138–145
- Buck RD (1963) Some applications of mechanics to the treatment of panel paintings. *Recent Advances in Conservation*, Thompson editor, London
- Hoadley B (1969) Perpendicular-to-grain compression set induced by restrained swelling. *Wood Science* 3:159–166
- Hoadley B (1995) Chemical and physical properties of wood. In: Dardes K, Rothe A (eds) *The structural conservation of panel paintings: proceedings of a symposium at the J. Paul Getty Museum*, The Getty Conservation Institute, Los Angeles, USA
- Hunt DG (1999) A unified approach to creep of wood. *Proc R Soc Lond A* 455:4077–4095
- Hunt DG, Shelton CF (1988) Longitudinal moisture-shrinkage coefficients of softwood at the mechano-sorptive creep limit. *Wood Sci Technol* 22:199–210
- Krauss A (2004) Swelling pressure of spruce wood along the grains moistened in humid air or water. *Folia Forestalia Polonica* 35:13–22

- Mazzanti P, Togni M, Uzielli L (2012) Drying shrinkage and mechanical properties of poplar wood (*Populus alba* L.) across the grain. *J Cult Herit* 13:S85–S89
- Mishiro A (1976) Studies on the swelling pressure of wood. Part VII: on the swelling pressure and relaxation of wood. *Mokuzai Gakkaishi* 22:129–132
- Mishiro A (1988) A consideration on the measuring method of swelling stress in wood. *Bull Tokyo Univ For* 79:113–118
- Molinski W, Raczkowski J (1988) Mechanical stresses generated by water adsorption in wood and their determination by tension creep measurements. *Wood Sci Technol* 22:193–198
- Perkitny T (1961) The swelling pressure of wood (In French). *Bois et forêts des tropiques* 80:39–49
- Perkitny T, Kingston RS (1972) Review of the sufficiency of research on the swelling pressure of wood. *Wood Sci Technol* 6:215–229
- Preziosa C, Guitard D, Sales C (1986) Internal stresses in wood: the tensor of the stress drying coefficients as an isotropic characteristic of the material (In French), *Bois et Forêt des Tropiques. Cahiers Scientifiques* 8:93–109
- Rybarczik W, Ganowicz R (1974) A theoretical description of the swelling pressure of wood. *Wood Sci Technol* 8:233–241
- Simpson WT, Skaar C (1968) Effect of restrained swelling on wood moisture content. US department of agriculture, Forest service, Forest Product Laboratory
- Svensson S, Toratti T (2002) Mechanical response of wood perpendicular to grain when subjected to changes of humidity. *Wood Sci Technol* 36:145–156
- Takahashi A, Schniewind AP (1974) Deformation and drying set during cyclic drying and wetting under tensile loads. *Mokuzai Gakkaishi* 20:9–14
- Tiemann DH (1942) *Wood technology*. Pitman Publishing Corporation, New York
- Uzielli L (1995) Historical overview of panel making techniques in central Italy. In: Dardes K, Rothe A (eds) *The Structural Conservation of Panel Paintings: Proceedings of a symposium at the J. Paul Getty Museum, The Getty Conservation Institute, Los Angeles, USA*
- Virta J, Koponen S, Absetz I (2005) Cupping of wooden cladding boards in cyclic conditions—a study of boards made of Norway spruce (*Picea abies*) and Scots pine (*Pinus sylvestris*). *Wood Sci Technol* 39:431–438
- Virta J, Koponen S, Absetz I (2006) Measurement of swelling stresses in spruce (*Picea abies*) samples. *Build Environ* 41:1014–1018